doi:10.14311/ppt.2023.1.28
Plasma Physics and Technology **10**(1):28–31, 2023

OPTICAL DIAGNOSTICS OF ANODE SURFACE TEMPERATURE IN VACUUM INTERRUPTERS WITH DIFFERENT CuCr COMPOSITIONS

N. Dorraki*, R. Methling, S. Gortschakow

Leibniz Institute for Plasma Science and Technology, Felix-Hausdorff-Str. 2 , 17489 Greifswald, Germany

* naghme.dorraki@inp-greifswald.de

Abstract. The requirements for contact material in vacuum interrupters are demanding because the arc medium is formed by electrode evaporation during the operation. Copper chromium alloy (CuCr) is widely used as contact material. Different compositions could result in a different rate of successful interruption. This work compares vacuum arc properties for two CuCr compositions - 75/25 and 50/50 weight percent. The contact surface temperature is measured during and after the vacuum arc with an AC current flow at 2 kA magnitude. Quantitative characterization of the contact surface temperature was obtained with near-infrared spectroscopy using Planck curve fitting and spectrally filtered high-speed photography. Evaluation of the anode surface temperature has shown a slower surface cooling for CuCr 50/50 compared to 75/25. Despite this, CuCr 75/25 has experienced higher temperature with dispersion in a larger area during the arcing time, in a successful current interruption.

Keywords: vacuum arc, optical diagnostics, surface temperature.

1. Introduction

Vacuum interrupters are superior types of circuit breakers particularly in medium voltage power-distribution systems, due to their efficiency and reliability, which stem from fast recovery time, a high number of operations, and safe, maintenance-free operations. The key to their operation is the formation of arc in metal vapour emitted from the contact surface. Following current zero, the dielectric gap can be rapidly recovered, unless the re-ionization of metal vapour in the medium under the influence of the transient recovery voltage (TRV) occurs. Therefore, the breaking capacity of vacuum interrupters is dependent on the properties and manufacturing technology of the electrode material. The main reasons for overheating the contacts in vacuum interrupters are: (i) the formation of anode spots, which causes the local melting of the anode surface and (ii) clustering of cathode spots, leading to enhanced cathode surface heating and an increase in metal vapour production in the contacts gap, which can result in arc reignition after current zero. These phenomena are particularly relevant for high-current arcs and are influenced by the properties of the electrode material, especially by its electrical and thermal conductivity [1].

Copper chromium alloy (CuCr) shows the optimal behaviour in several aspects for vacuum interrupters, e.g. mechanical strength, thermal stability and erosion behaviour. This enables the vacuum interrupters to withstand high electrical and thermal loads [2].

The aim of this paper is to examine the interaction between vacuum arc and the electrodes by determining the anode surface temperature for two CuCr compositions, namely 75/25 and 50/50 (weight percent). To accomplish this goal, near-infrared (NIR) spectroscopy and high-speed photography enhanced by a narrow-band filters are employed to measure the anode surface temperature during the arcing and after the current interruption.

2. Experimental setup

The setup includes a model vacuum interrupter connected to a high-current generator. The vacuum chamber is equipped with glass windows, which enable optical diagnostics of the arc and electrodes [3].

2.1. The model vacuum interrupter

The setup schematically shown in Figure 1 was used in experiments. The CuCr electrodes are enclosed in a vacuum chamber which is evacuated to a pressure level below 10^{-6} mbar. The electrodes are positioned vertically. The anode, connected to the current generator, remains stationary and is fixed on top of the chamber, while the lower electrode is the movable cathode. The cathode is connected to a pneumatic-driven actuator that enables an opening speed of about 1 m/s. The CuCr electrodes are cylindrically shaped with a diameter of 10 mm with two conventionally used compositions of 75/25 and 50/50 percent by weight. The experiments are carried out with an AC current of 2 kA peak measured by a Rogowski coil (PEM CWT 1500). The arc voltage is measured using a voltage probe (Tektronix P6015A).

2.2. Electrical diagnostics

Figure 2 shows the waveforms of measured arc current and voltage for the two compositions of CuCr. The arc is initiated in both cases approximately at the same time, $t_0 = 1.1$ ms. The arc voltage for both waveforms is similar until the instant $t_1 = 4$ ms, when a jump of a few volts, which shows the formation of an anode spot, occurs. In case of CuCr 50/50 mostly the

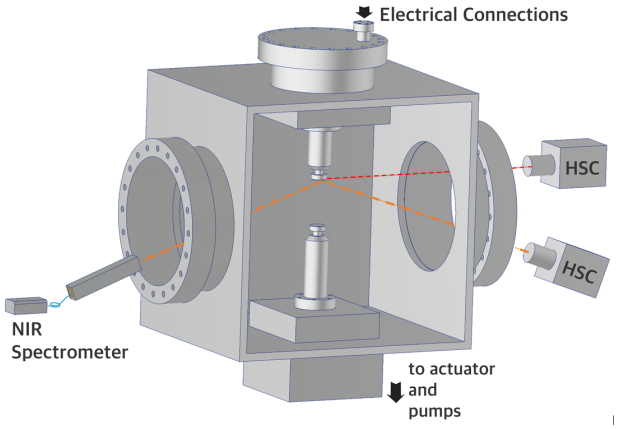

Figure 1. Schematic view of the vacuum chamber with positions of NIR spectrometer and high-speed cameras (HSC).

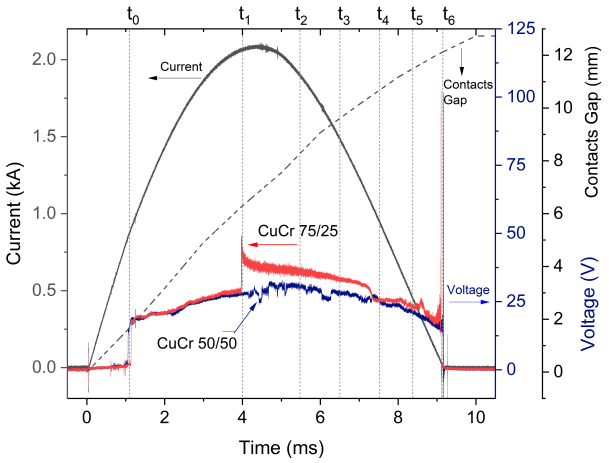

Figure 2. Current and voltage waveforms, and the contact travel curve(dashed line, 0–12.7 mm)

anode spot of type 1 has been obtained. CuCr 75/25 has shown a stable formation of the anode spot of type 2, which is characterized by higher voltage jump. The current is interrupted after the first current zero crossing (instant t_6).

2.3. Optical diagnostics

The anode surface temperature is analysed using an NIR spectrometer and spectrally filtered high-speed photography, after current zero and during the arcing period, respectively. The NIR spectroscopic setup consists of a compact spectrometer (Hamamatsu C1142GA, wavelength range of 900-1700 nm) and a focusing setup that images the centre of the anode spot with a spatial size of about 1 mm^2 to the spectrometer (Figure 1). The spectra are recorded after the instant of current maximum. The temperature evaluation was performed for the instants after arc interruption to avoid the impact of arc radiation. An exposure time of 200 µs and a temporal resolution of 1.25 ms have been used. After the acquisition, the spectra are calibrated to obtain absolute intensity using a tungsten strip lamp. Subsequently, the spectra are processed by comparing the measured radiances to the black body emission according to Plank law with the aim of determining the temperature of the anode surface. The detailed methodology is outlined in [3, 4].

The anode surface temperature before the current zero is obtained using a high-speed camera (Integrated Design Tools, type Y4) equipped with a multilayer interference filter (MIF) having maximum transmission at 891 nm and FWHM of 10 nm. The recording speed was 10,000 frames per second with an exposure time of 1 µs. The filter selection is made in such a way that the contribution of plasma radiation is minimized. Therefore, the recorded emission can be attributed to the thermal emission of the anode surface.

To obtain the temperature profile of the anode surface during the arc, a correlation between high-speed thermography and NIR spectroscopy is required. However, differentiating between the thermal emission of the anode surface and arc emission is challenging when the intensity of arc emission is high. Consequently, the frames and spectra captured close to the instant of current interruption are used to establish a correlation between the absolute temperature, as measured by NIR spectroscopy at a specific position on the anode, and the emission intensity recorded by high-speed photography. The detailed calibration method for surface temperature distribution can be found in [4].

In addition to measurements for determination of the anode surface temperature, the dynamic of the vacuum arc is also recorded during the operation using a high-speed camera (Integrated Design Tools, type Y6) with the same recording speed as the thermography. By synchronizing the two high-speed cameras, it is feasible to monitor arc ignition, shape, and movement while evaluating the temperature distribution of the anode surface. In such cases, corrections could be applied to the recorded frames of the anode surface for reducing the impact of arc radiation on temperature measurement.

3. Results

3.1. Surface temperature after current interruption

The surface temperature measurement by NIR spectroscopy after current interruption is performed for more than 20 tests under similar conditions, with a peak current of 2 kA and an arc duration of 8 ± 0.2 ms. The temperature measurements are taken for a spot with an area of about 1 mm^2 located at the centre of the anode spot. The temperature averaged over all tests is presented in Figure 3. The time zero corresponds to the instant of current interruption. Plank curve fitting is executed for all the measurements after the current interruption. For the instants during the arcing, the temperature is estimated for the very last spectra before current zero only, where the contribution of plasma radiation to the measured optical

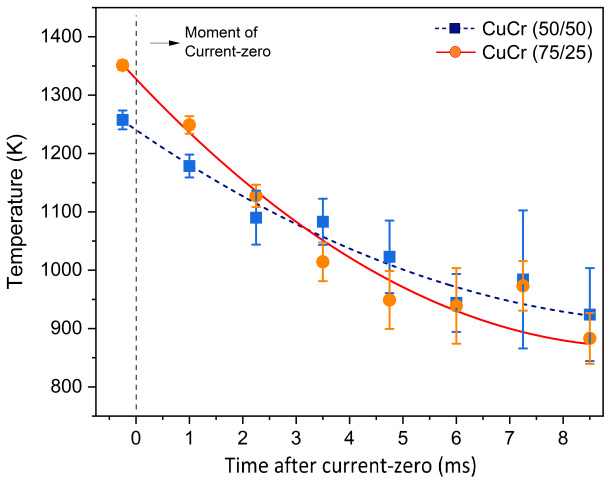

Figure 3. Temporal evolution of averaged anode surface temperature measured after current interruption for CuCr 75/25 and 50/50.

signal can be considered as negligible. For temperatures measured below 1000 K, uncertainties of no less than ±50 K have been reported [4]. The Plank curve fitting technique relies on two independent parameters, namely temperature and emissivity. Notably, for lower temperatures, higher uncertainties in emissivity are observed, and vice versa. Thus, it could be possible that the error bars exceeding ±50 K stem from uncertainties in emissivity and the signal-to-noise ratio, which could arise during the post-processing stage. Therefore, the determination of temperatures less than 900 K is neglected due to high uncertainties in the measurements.

3.2. Surface temperature distribution during arcing

Temporal evolution of anode surface temperature during arcing was determined using high-speed photography enhanced by MIF. This technique, however, has some deficits in the case when an intense arc radiation occurs and the contacts gap is relatively small. This typically happens before the instant of current maximum. Therefore, for the sake of accuracy, the anode temperature evolution after the peak current until the instant of current zero crossing was considered for the measurements by high-speed camera. The temperature profiles of the anode surface are exemplarily shown in Figure 4 for two cases. The corresponding voltage waveforms and the instants of temperature profile evaluation ($t_2 - t_5$) are presented in Figure 2. The dashed circle shows the anode boundary.

Comparing the temperature profiles of the two compositions of CuCr, a higher temperature for CuCr 75/25 for the same level of current was observed. However, the surface cooling rate is faster for CuCr 75/25, similar to what is inferred from the temporal evolution of temperature after current zero (Figure 3).

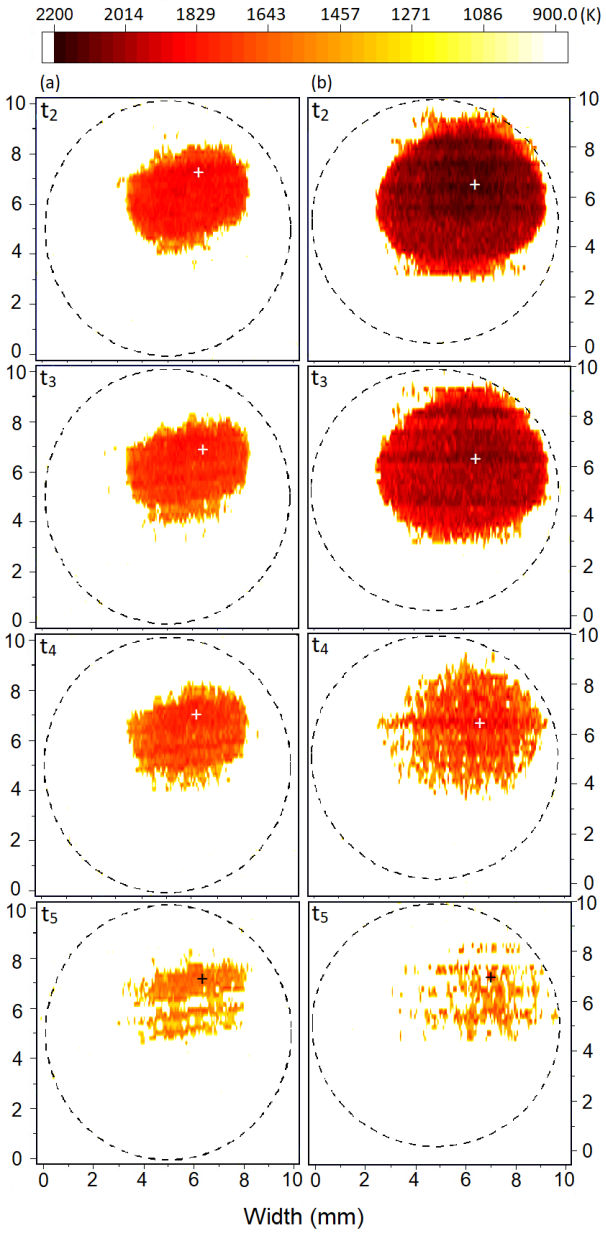

Figure 4. Anode temperature profiles for the instants at $t_2 - t_5$ for two different compositions of CuCr; a) 50/50 and b) 75/25. The mark (+) shows the position of maximum temperature.

4. Discussion

After the current interruption, heat transfer through convection is not possible any more. The heat stored in the electrode can only be lost by radiation from the contact surface and by conduction inside the contact body. Therefore, a high thermal conductivity is preferable for cooling down the contacts. Previous studies have shown that CuCr alloys with higher Cr percentages have lower thermal conductivities than those with lower percentages of Cr [5, 6]. Therefore, the CuCr 75/25 alloy is expected to have higher heat transfer efficiency in a larger dissipation area. This is consistent with the results shown in Figure 3, where the temperature of CuCr 75/25 decreases faster than

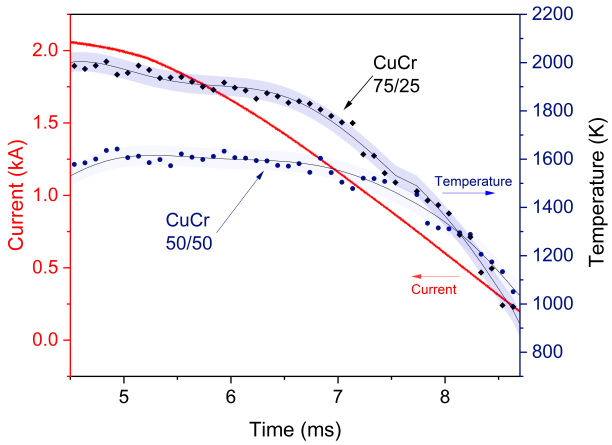

Figure 5. Temporal evolution of average temperature of anode surface above 900 K for CuCr 75/25 and 50/50.

that of CuCr 50/50. On the other hand, a reduction of Cr content in the alloy decreases the CuCr melting point. This can lead to enhanced probability of anode spot type 2 formation in the high-current regime. Anode spot formation can force a local current density enhancement (due to the arc constriction) and localised heating, causing a strong surface melting and formation of significant liquid pool. As a result, the molten area may become overheated due to Joule heating by increasing current. As mentioned before, the higher voltage jump in the arc voltage waveform at 4 ms (t_1) for CuCr 75/25 presented in Figure 2 shows an anode spot type 2 formation. Therefore, the high temperature recorded at t_2 for CuCr 75/25 is caused by the formation of this specific anode mode, even though the thermal conductivity of CuCr 75/25 is higher than that of CuCr 50/50. By comparing the voltage waveforms of a high number of tests conducted on two different compositions of CuCr, it is observed that the possibility of anode spot type 2 formation is significantly higher in CuCr 75/25 compared to CuCr 50/50. In the case of lower Cr content this probability was almost at 100%, while it was below 35% for CuCr 50/50.

To analyse the temporal evolution of surface temperature distribution, the mean temperature is determined for the area limited to the temperature above 900 K (Figure 5). It is noteworthy that in the vicinity of the current zero, the temperature distribution of CuCr 75/25 displays a greater dispersion compared to that of CuCr 50/50. Experimental studies using small-sized contacts have shown that the rate of interruption failure increases with a higher Cr content in the alloy, even at low current levels [7]. The results obtained in this project suggest that this failure could be attributed to a slower cooling rate of contact surfaces for CuCr with a higher percentage of Cr, despite CuCr with lower chromium content could experience higher temperatures during arcing because of the higher possibility of anode spot formation.

Taking into account the current density, it is important to note that the findings of this study with reduced-size contacts operating at a current of 2 kA can be extended to vacuum arcs with bigger contacts in diameter and higher current levels.

5. Conclusions

The present study has employed optical techniques to measure the anode surface temperature of two CuCr compositions during and after the vacuum arc. The results show that anode surface cooling down is slower for CuCr 50/50 compared to 75/25. This could be a potential reason of higher number failure in interruption for high content of chromium in CuCr. However, CuCr 75/25 experienced higher temperature in larger area during arcing time because of anode spot formation.

It is important to note that the findings of this study are confined to contacts of reduced size while the arc has a fixed position on the electrode to investigate the influence of different compositions of CuCr by optical techniques. Other parameters, such as different contact design and electrode material manufacturing by different methods, should be considered for future studies.

Acknowledgements

This research was funded by the Deutsche Forschnungsgemeinschaft (DFG, German Research Foundation) project GO 3402/1-1.

References

[1] P. G. Slade. *The vacuum interrupter: theory, design, and application*. CRC press, 2018.

[2] P. G. Slade. *Electrical contacts: principles and applications*. CRC press, 2017.

[3] S. Gortschakow, S. Franke, R. Methling, et al. Advanced optical diagnostics for characterization of arc plasmas. *IEEE Transactions on Plasma Science*, 49(9):2505–2515, 2021. doi:10.1109/TPS.2021.3096289.

[4] R. Methling, S. Franke, S. Gortschakow, et al. Anode surface temperature determination in high-current vacuum arcs by different methods. *IEEE Transactions on Plasma Science*, 45(8):2099–2107, 2017. doi:10.1109/TPS.2017.2712562.

[5] X. Huang, L. Wang, S. Jia, et al. Numerical simulation of thermal characteristics of anodes by pure metal and CuCr alloy material in vacuum arc. *IEEE Transactions on Plasma Science*, 43(8):2283–2293, 2015. doi:10.1109/TPS.2015.2443811.

[6] W. Li, R. Thomas, and R. Smith. Effects of Cr content on the interruption ability of CuCr contact materials. *IEEE Transactions on Plasma Science*, 29(5):744–748, 2001. doi:10.1109/27.964467.

[7] D. Heyn, M. Lindmayer, and E.-D. Wilkening. Effect of contact material on the extinction of vacuum arcs under line frequency and high frequency conditions. *IEEE transactions on components, hybrids, and manufacturing technology*, 14(1):65–70, 1991. doi:10.1109/33.76512.